Supplementary Materials for

Dual-Strong Ligand Intervention for Extreme-Condition Aqueous Zn Batteries

Ruizhi Zhang [a, b, c]†, Wangwu Li [a]†, Qiong Cai [b], Wei Kong Pang [c], Jitraporn (Pimm) Vongsvivut [d], Jingxiu Wang [a], Cheng Zhang [e], Jodie A. Yuwono [a]*, Sailin Liu [a]* and Zaiping Guo [a, f]*

a. School of Chemical Engineering, The University of Adelaide; Adelaide, SA 5005, Australia.
b. School of Chemistry and Chemical Engineering, University of Surrey; Guildford, Surrey GU2 7XH, United Kingdom.
c. Institute for Superconducting & Electronic Materials, University of Wollongong; Wollongong, NSW 2500, Australia.
d. Australian Synchrotron, Australia's Nuclear Science and Technology Organization, Clayton VIC 3168, Australia.
e Australian Institute for Bioengineering and Nanotechnology, the University of Queensland, St Lucia QLD 4067, Australia.
f. Department of Materials Science and Engineering, City University of Hong Kong, Kowloon, Hong Kong 999077, China

†*These authors contribute equally to this work*
**Corresponding author:* jodie.yuwono@adelaide.edu.au, sailin.liu@adelaide.edu.au, zaiping.guo@adelaide.edu.au

Content

Table S1 The ESP_{min} and ESP_{max} values of solvents.

	ESP_{max} (eV)	ESP_{min} (eV)
DMMP	0.98912	−2.08968
TEP	0.623133	−2.03808
TMP	0.765365	−1.99645
DMAC	0.915402	−1.91536
urea	1.930107	−1.8772
DMF	0.91627	−1.87243
PC	1.392834	−1.73107
H_2O	1.860725	−1.7211
Gly	2.146924	−1.65909
IPA	1.713289	−1.58407
EtOH	1.784406	−1.58016
DMK	0.808728	−1.5793
MEK	0.783144	−1.57539
G1	0.486104	−1.25581
G2	0.49868	−1.24627

DMMP: dimethyl methyl phosphonate.
TEP: triethyl phosphate.
TMP: trimethyl phosphate.
DMAC: N,N-dimethylacetamide;
DMF: dimethylformamide.
PC: propylene carbonate.
IPA: isopropanol alcohol
Gly: glycerol.
EtOH: ethanol.
DMK: acetone.
MEK: methyl ethyl ketone.
G1; 1,2-dimethoxyethane.
G2: diethylene glycol dimethyl ether.

Table S2 Binding energy ($\triangle E_b$) of H_2O-solvents.

	Binding Energy (eV)
H_2O-DMMP	−0.382656
H_2O-TEP	−0.388374
H_2O-TMP	−0.312236
H_2O-DMAC	−0.21924
H_2O-DMF	−0.264456
H_2O-urea	−0.521791
H_2O-PC	−0.11580
H_2O-H_2O	−0.331776
H_2O-Gly	−0.397984
H_2O-IPA	−0.247705
H_2O-EtOH	−0.217119
H_2O-DMK	−0.23152
H_2O-MEK	−0.177615
H_2O-G1	−0.181207
H_2O-G2	−0.179284

Table S3 Ratio of complexes in electrolytes.

Electrolyte	Complex	Ratio
AE	$Zn^{2+}(H_2O)_6$	0.83
	$Zn^{2+}(H_2O)_5(OTf^-)$	0.11
	$Zn^{2+}(H_2O)_4(OTf^-)_2$	0.06
HE	$Zn^{2+}(H_2O)_4(DMMP)_1(OTf^-)_1$	0.28
	$Zn^{2+}(H_2O)_3(DMMP)_1(OTf^-)_2$	0.12
	$Zn^{2+}(H_2O)_5(DMMP)_1$	0.12
	$Zn^{2+}(H_2O)_6$	0.12
	$Zn^{2+}(H_2O)_4(DMMP)_2$	0.12
	$Zn^{2+}(H_2O)_5(OTf^-)$	0.12
	$Zn^{2+}(H_2O)_4(OTf^-)_2$	0.08
	$Zn^{2+}(H_2O)_3(DMMP)_2(OTf^-)_1$	0.04
UHE	$Zn^{2+}(H_2O)_4(urea)_1(DMMP)_1$	0.13
	$Zn^{2+}(H_2O)_2(urea)_2(DMMP)_1(OTf^-)_1$	0.13
	$Zn^{2+}(H_2O)_5(urea)_1$	0.08
	$Zn^{2+}(H_2O)_5(DMMP)_1$	0.08
	$Zn^{2+}(H_2O)_5(urea)_1$	0.08
	$Zn^{2+}(H_2O)_3(DMMP)_2(OTf^-)_1$	0.04
	$Zn^{2+}(H_2O)_3(urea)_1(DMMP)_2$	0.04
	$Zn^{2+}(H_2O)_2(urea)_1(DMMP)_2(OTf^-)_1$	0.04
	$Zn^{2+}(H_2O)_4(DMMP)_1(OTf^-)_1$	0.04
	$Zn^{2+}(H_2O)_2(DMMP)_3(OTf^-)_1$	0.04
	$Zn^{2+}(H_2O)_2(urea)_3(OTf^-)_1$	0.04
	$Zn^{2+}(H_2O)_4(OTf^-)_2$	0.04
	$Zn^{2+}(H_2O)_3(urea)_1(OTf^-)_2$	0.04
	$Zn^{2+}(H_2O)_2(urea)_2(OTf^-)_2$	0.04
	$Zn^{2+}(H_2O)_5(OTf^-)$	0.04
	$Zn^{2+}(H_2O)_4(urea)_1(OTf^-)_1$	0.04
	$Zn^{2+}(H_2O)_2(urea)_1(OTf^-)_1$	0.04

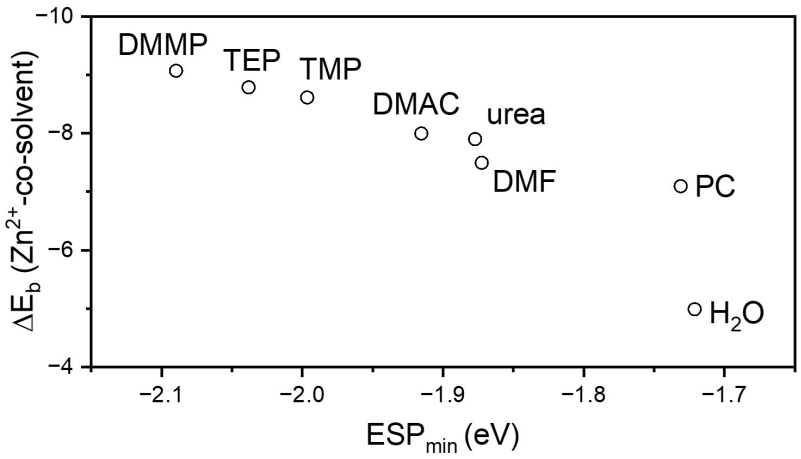

Fig. S1 Binding energy ($\triangle E_b$) of Zn^{2+}-solvents.

DMMP, dimethyl methyl phosphonate; TEP, triethyl phosphate; TMP, trimethyl phosphate; MAC, N,N-dimethylacetamide; DMF, dimethylformamide; PC, propylene carbonate;

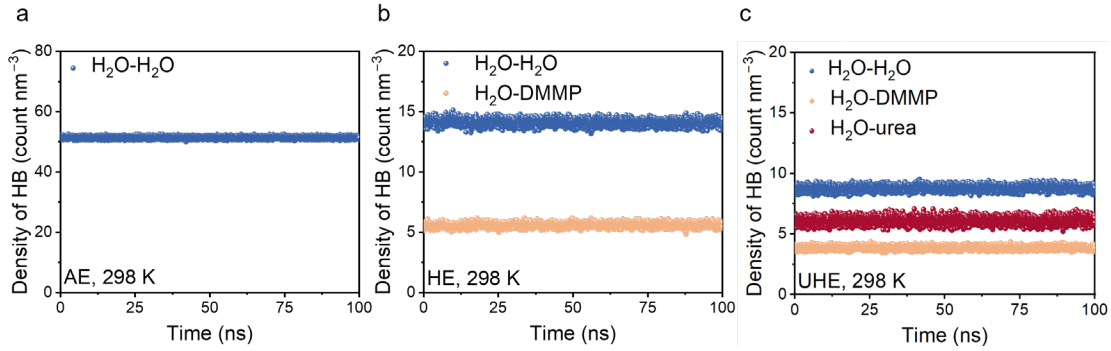

Fig. S2 Density of hydrogen bond in electrolytes.

Density of hydrogen bond between H_2O-H_2O, H_2O-DMMP, H_2O-urea in (a) AE, (b) HE, and (c) UHE electrolytes at 298 K.

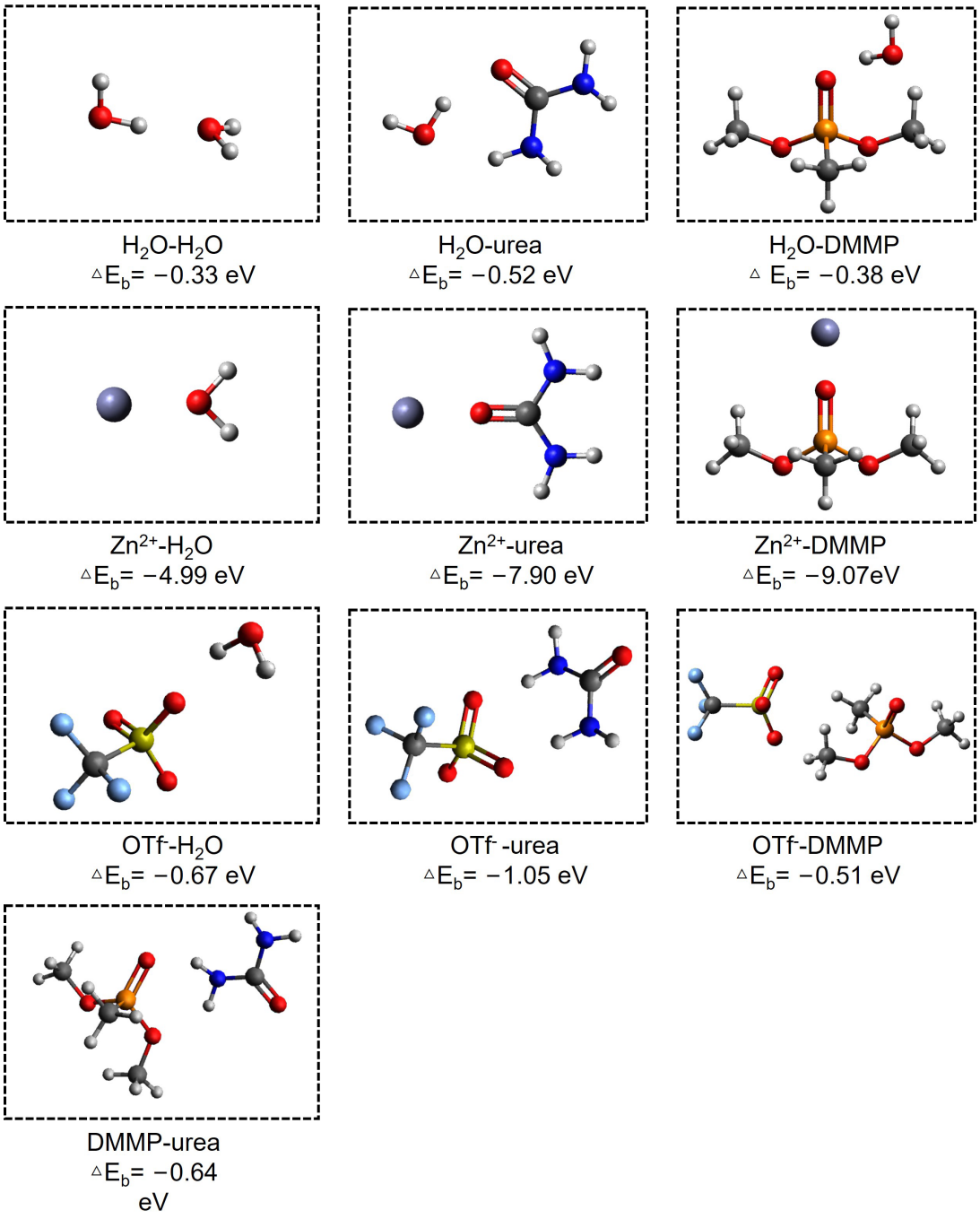

Fig. S3 Geometries of components for DFT calculation of $\triangle E_b$.

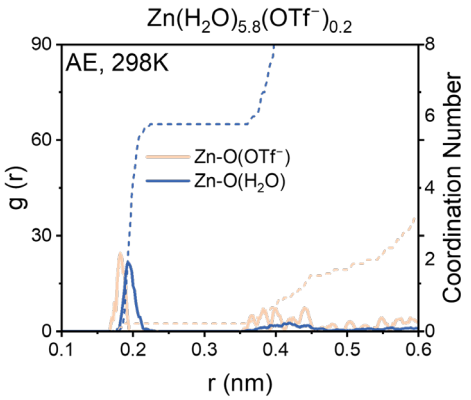

Fig. S4 RDF and CN of Zn^{2+} with O from OTf^- and H_2O in AE.

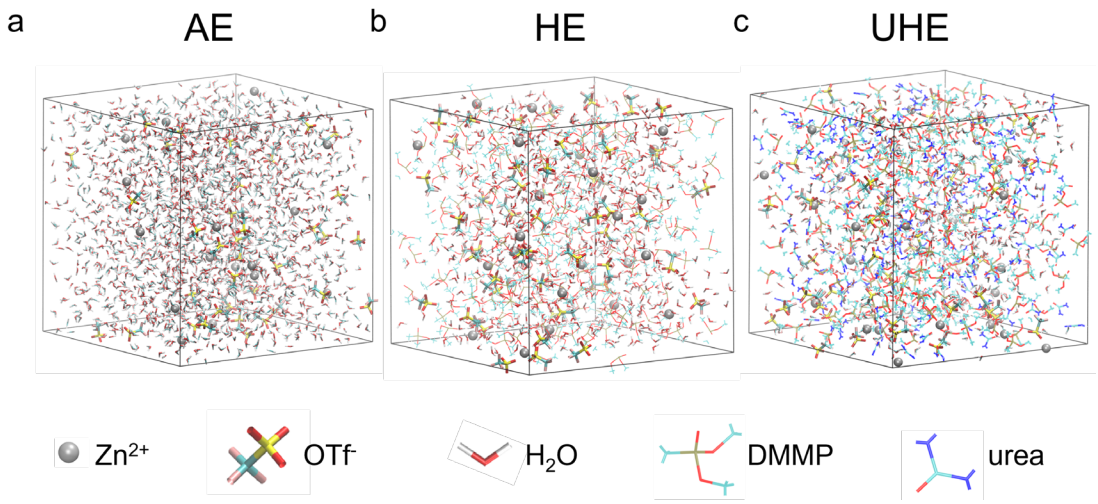

Fig. S5 MD simulation snapshot.
Snapshot of the MD simulation boxes of (a) AE, (b) HE, and (c) UHE electrolytes.

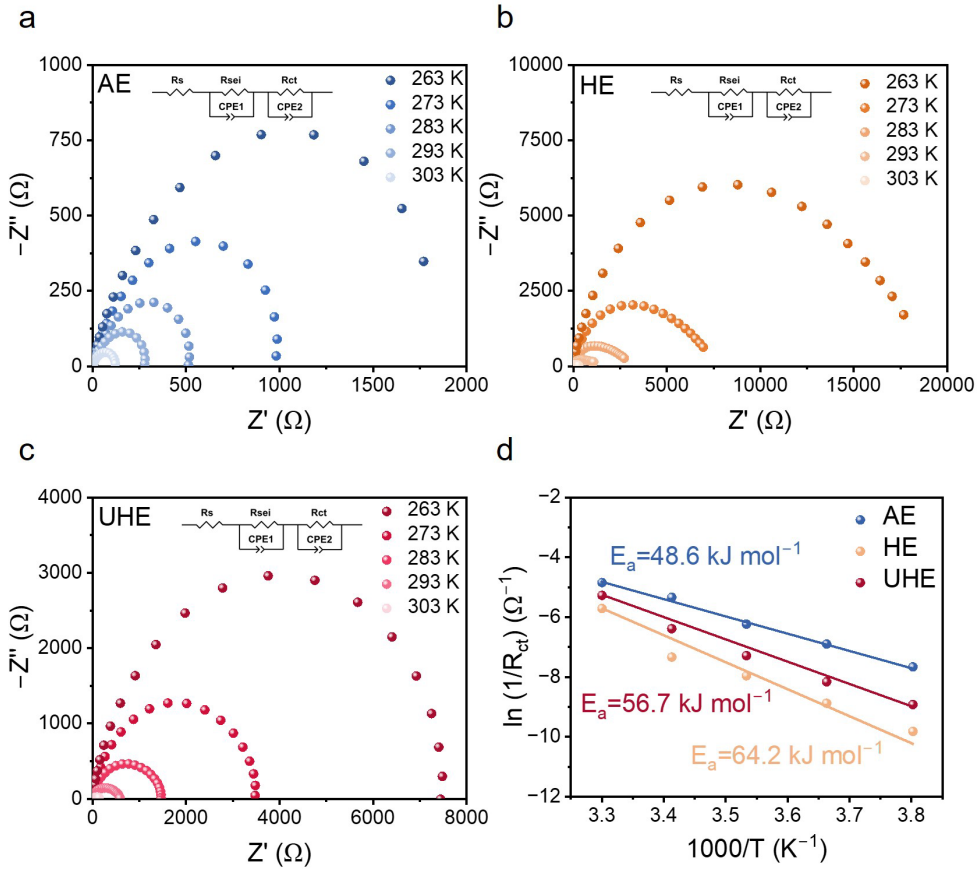

Fig. S6 Nyquist plots for Zn//Zn cells at varying temperatures.

Nyquist plots for Zn//Zn cells in (a) AE, (b) HE, and (c) UHE electrolytes at 263 K, 273 K, 283 K, 293 K, 303 K. Insets show the equivalent circuit model used for fitting (d) Arrhenius behaviour of Zn^{2+} desolvation in the electrolytes and the desolvation energy (E_a).

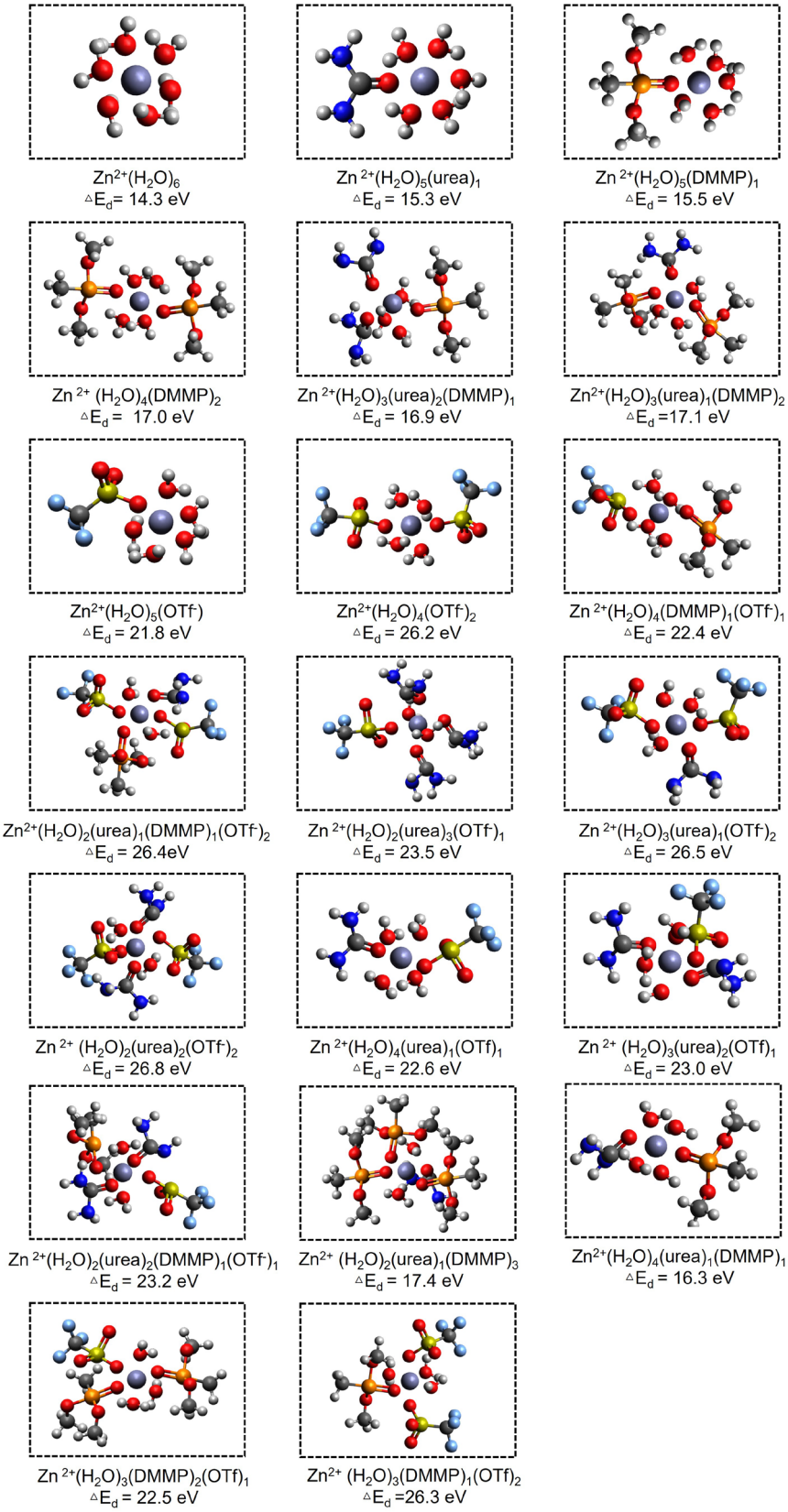

Fig. S7 Geometries of the $Zn^{2+}(H_2O)_x(urea)_y(DMMP)_z(OTf^-)_{6-x-y-z}$ complexes for DFT calculation of $\triangle E_d$.

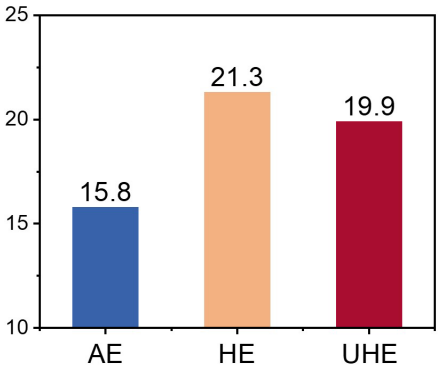

Fig. S8 Desolvation energy ($\triangle E_{des}$) of Zn^{2+} in electrolytes from an integrated study of MD simulations and DFT calculations.

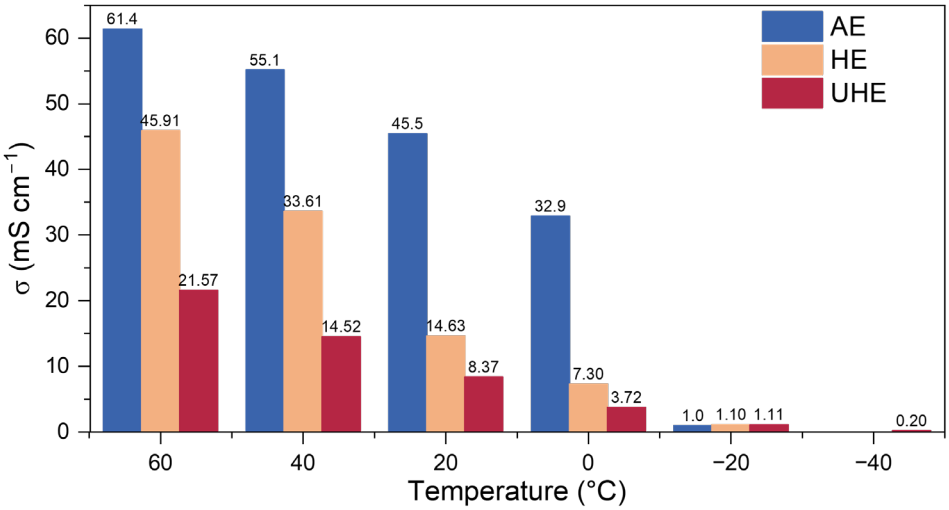

Fig. S9 Ionic conductivity of electrolytes.
Ionic conductivity of electrolytes at −40, −20, 0, 20, 40, 60°C.

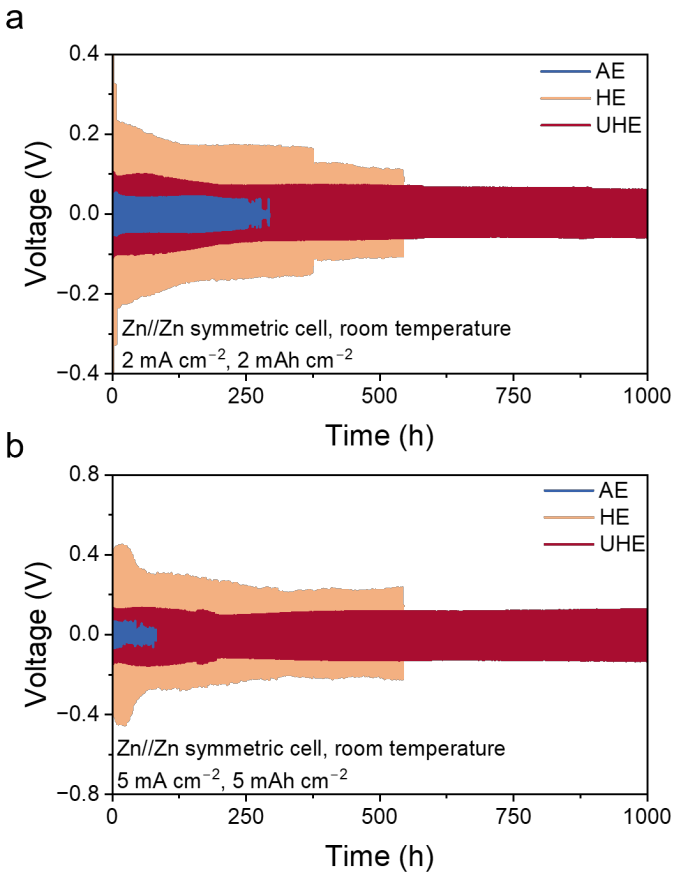

Fig. S10 Cycling performance of Zn//Zn symmetric cells at room temperature. Voltage profiles of galvanostatic plating/stripping of Zn//Zn symmetric cells with AE, HE, and UHE electrolytes at current density of (a) 2 mA cm^{-2}, areal capacity of 2 mAh cm^{-2} and (b) 5 mA cm^{-2}, areal capacity of 5 mAh cm^{-2} at room temperature.

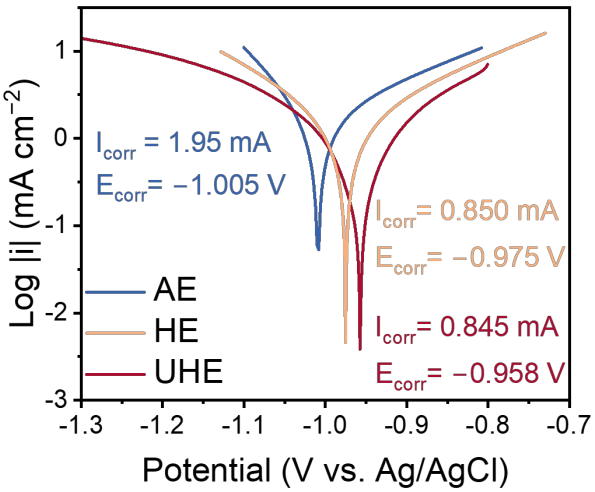

Fig. S11 Tafel plots of Zn electrode in electrolyte.

Tafel plots of Zn electrode in electrolyte and corresponding corrosion potential (E_{corr}) and corrosion current (I_{corr}).

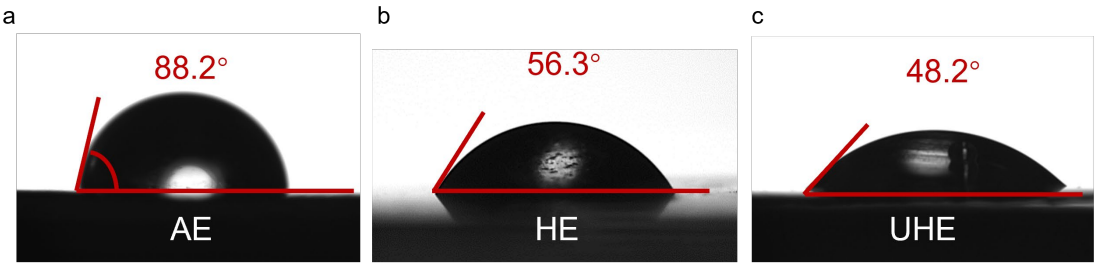

Fig. S12 Contact angles.
Contact angles of (a) AE, (b) HE, and (c) UHE electrolytes on pristine Zn.

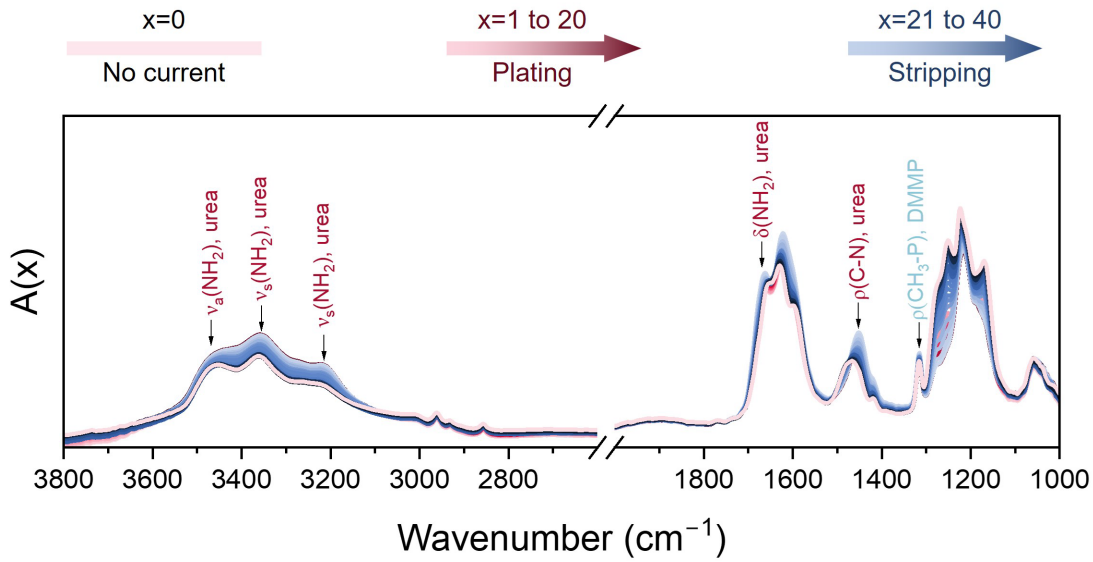

Fig. S13 In-situ FTIR spectra collected during Zn electroplating/stripping in UHE.

In situ FTIR spectra were collected continuously during the Zn plating/stripping process.

[A(0)]: The lightest red line represents the spectrum of electrolyte as no current is applied.

[A(x)], where x ranges from 1 to 20: The lines with the colors changing from light red to dark red were collected during the Zn plating process. They provide information on the Zn^{2+} desolvation process and the state of the electrode/electrolyte interphase during Zn plating.

[A(x)], where x ranges from 21 to 40: The lines with the colors changing from light blue to dark blue were collected during the Zn stripping process. They provide information on Zn^{2+} solvation process and the state of the electrode/electrolyte interphase during Zn stripping.

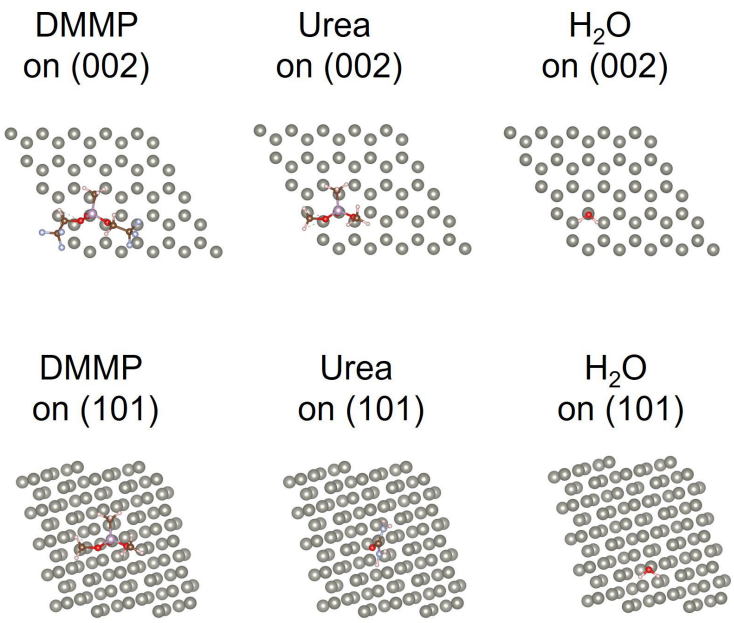

Fig. S14 Top view of the adsorption models of DMMP, urea, and H_2O on the (002) and (101) crystal planes.

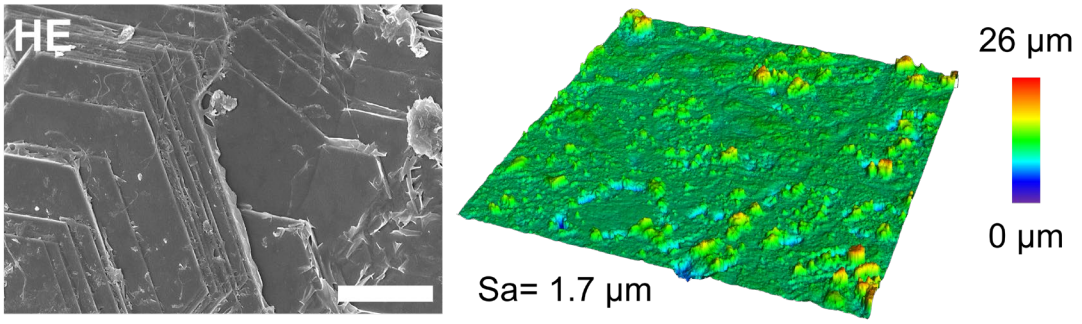

Fig. S15 SEM and 3D reconstruction image of Zn electrodes cycled in HE electrolyte.

SEM image (bar=2 μm), 3D reconstruction image, and S_a value of Zn electrodes cycled in HE electrolyte at 1 mA cm^{-2}, 1 mAh cm^{-2} for 20 times.

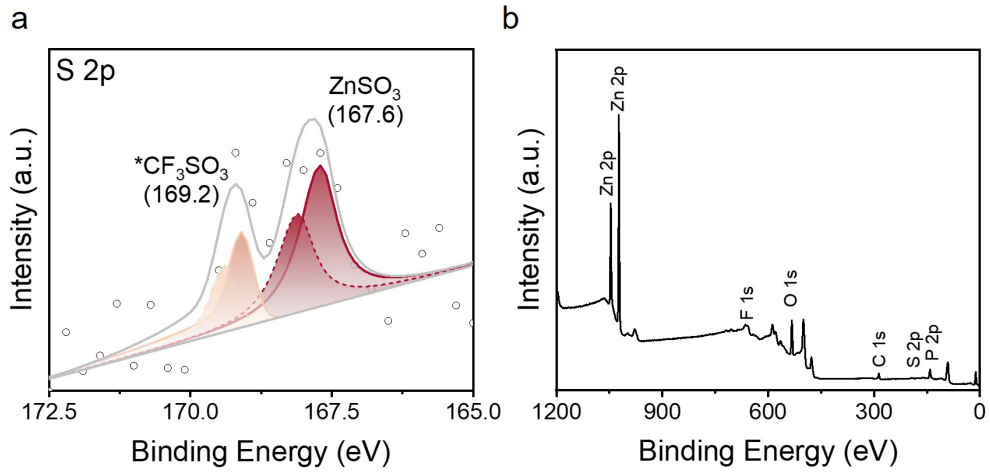

Fig. S16 XPS analysis of Zn anode cycled in the UHE electrolyte.

(a) XPS spectra of S 2p and (b) XPS full spectrum of Zn anode cycled in the UHE electrolyte after 20 times at 1 mA cm^{-2}, 1 mAh cm^{-2}

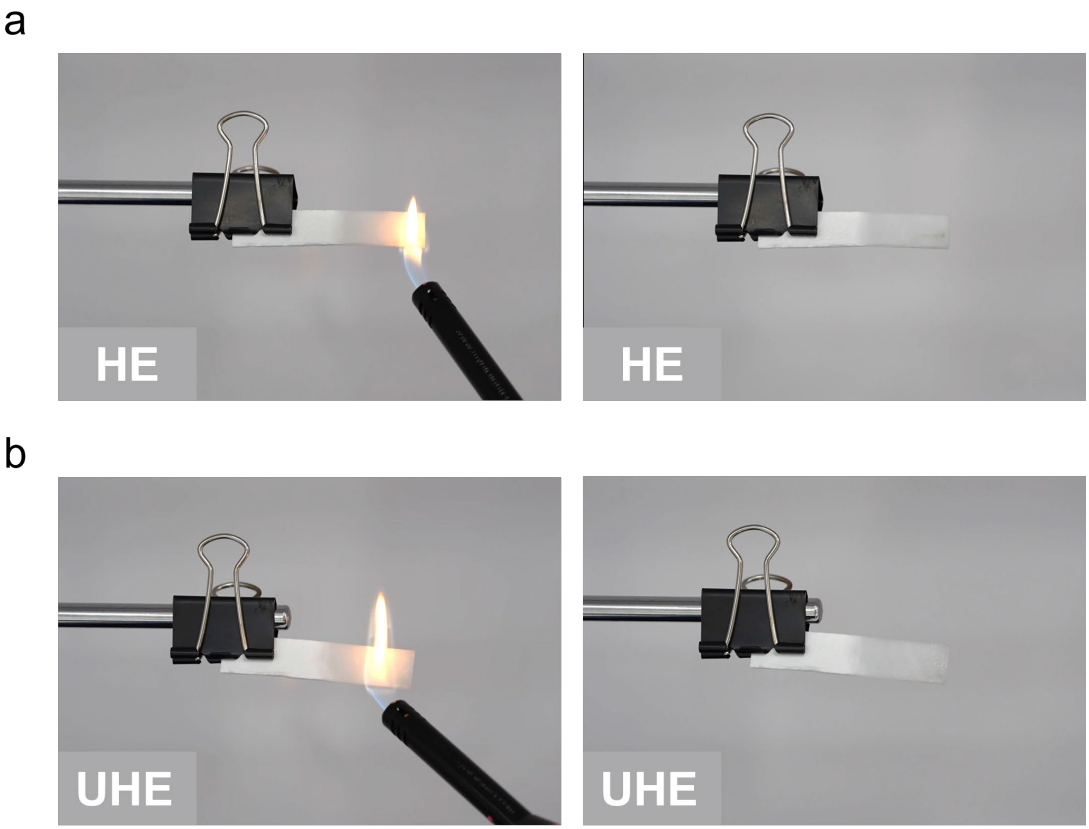

Fig. S17 Ignition test of (a) HE and (b) UHE electrolytes.

Digital images of ignition test for the (a) HE and (b) UHE electrolytes, showing that both are all non-flammable.